

Design and operation of LongBo: a 2 m long drift liquid argon TPC

**C. Bromberg^a, B. Carls^b, D. Edmunds^a, A. Hahn^b, W. Jaskierny^b, H. Jostlein^b,
C. Kendziora^b, S. Lockwitz^b, B. Pahlka^b, S. Pordes^b, B. Rebel^b, D. Shooltz^a,
M. Stancari^b, T. Tope^b and T. Yang^b**

^a*Michigan State University, East Lansing, Michigan 48824 USA*

^b*Fermi National Accelerator Laboratory, Batavia, Illinois 60510, USA*

ABSTRACT: In this paper, we report on the design and operation of the LongBo time projection chamber in the Liquid Argon Purity Demonstrator cryostat. This chamber features a 2 m long drift distance. We measure the liquid argon purity using cosmic ray muons and confirm the electron drift lifetime is at least 6 ms as measured using purity monitors. LongBo uses cold electronics with discrete circuitry for the preamplifiers, and we measure a signal-to-noise (S/N) ratio of 30 at a drift field of 350 V/cm. An ASIC version of the cold preamplifiers was implemented on 16 readout channels, and we measure a S/N ratio 1.4 times larger for these channels.

KEYWORDS: LArTPC.

Contents

1. Introduction	1
2. Construction of the LongBo TPC	2
3. The High Voltage System	3
4. Electronics	4
4.1 Cold Electronics	4
4.2 Signal to Noise Ratio	5
4.3 Trigger	7
5. Operation	7
6. Results	8
6.1 Measurement of Electron Attenuation Using Cosmic Ray Muons	8
6.2 High Voltage Stability	14
7. Conclusions	14

1. Introduction

Liquid argon time projection chambers (LArTPCs) provide excellent spatial and calorimetric resolutions for measuring the properties of neutrino interactions above a few MeV. Conventional liquid argon vessels are evacuated to remove water, oxygen and nitrogen contaminants present in the ambient air prior to filling with liquid argon. However, as physics requirements dictate larger cryogenic vessels to hold bigger detectors, the mechanical strength required to resist the external pressure of evacuation becomes prohibitively costly. The Liquid Argon Purity Demonstrator (LAPD) [1] was an R&D test stand at Fermilab designed to determine if electron drift lifetimes adequate for large neutrino detectors could be achieved without first evacuating the cryostat. The electron drift lifetime in this test measured with purity monitors was greater than 6 ms without initial evacuation of the cryostat; that lifetime exceeds the value of approximately 2 ms required for future large LArTPCs with drift distances on the scale of a few meters.

After achieving the required electron drift lifetimes, the LAPD cryostat was emptied and a TPC of 2 m drift distance, named LongBo, was installed in the central cryostat region. High liquid argon purity was achieved with the TPC in the tank. This paper summarizes the design and operation of the LongBo TPC, which was the first TPC operated in the US to achieve a drift distance of 2 m.

2. Construction of the LongBo TPC

The LongBo TPC has a cylindrical sensitive volume with a 25 cm diameter and a 2 m length. LongBo extended the drift distance of the “Bo” TPC that was made a few years earlier with a 50 cm length [2]. LongBo has three sense wire planes, with wires oriented at 60 degrees from each other. The wires are 4.7 mm apart and made of 125 micron diameter beryllium copper. They were hand-soldered to a 3 mm thick copper-clad G10 board for each plane. The copper cladding was routed in a pad pattern on a Fermilab CNC router. A set of individual wires (shown with white insulation in figure 1) were soldered to the readout boards and terminated in a connector matched to a corresponding one on the preamplifier motherboards. The preamplifiers, often referred to as “cold preamplifiers” since they operated in the 87 K liquid argon, were placed around the TPC just outside the field cage; an arrangement dictated by the size of the cryostat flange on which the TPC was mounted. Olefin insulated flat cables took the signals from the motherboards to the signal feedthrough. The planes were biased from external voltage sources via a feed through. The cathode was made from copper mesh, chosen to allow free argon flow along the TPC axis. The mesh was stretched inside a ring made of 19 mm diameter 3 mm thick stainless steel tube, which supports the TPC. A stainless steel tube elbow was welded to this ring and served to connect to the high voltage feed through, described in Section 3, via a cup and spring-finger connection.

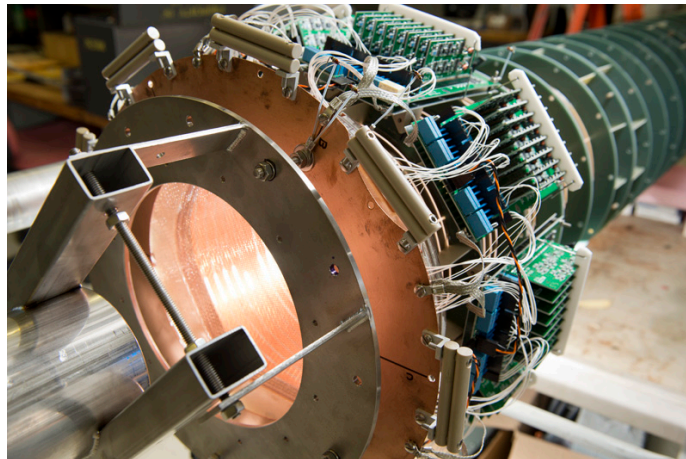


Figure 1: The wire planes and cold preamplifiers.

A uniform electric drift field was provided to the Bo TPC by a cylinder made of a copper-clad, 0.6 mm thick, G10 sheet, which is 50 cm long by 78 cm wide. The sheet was routed to create 18 mm wide copper strips, separated by 1.5 mm. The sheet was rolled into a 25 cm diameter tube which was inserted into a set of 7 rings routed from 4 mm thick G10. Two strings of 100 MOhm voltage divider resistors, Ohmite model 104, rated at 10 kV, 1 W, were soldered to the inner surface of the copper sheet. Only one string is necessary to create the electric field; the second is for redundancy. Figure 2 shows the resistors soldered to the inner surface of the copper sheet.

Bo was converted to LongBo by inserting three additional drift field sections, each 50 cm long, for a total drift length of 2 m. The drift field sections were connected together using threaded rod to make the full 2 m drift cage. Beryllium copper spring stock were soldered to the ends of each



Figure 2: The resistors soldered to the inner surface of the copper sheet.

cylinder to assure inter-connection at the joints. Figure 3 shows the assembled TPC with high voltage feedthrough and electronics.

3. The High Voltage System

To provide the electric field to drift the signal electrons, a high voltage was applied to the cathode mesh on the bottom of the TPC. The high voltage was generated outside of the cryostat by a Glassman LX150N12 power supply [3]. The supply was controlled remotely by a program and was set to trip if more than 1.1 mA of current was drawn. Before entering the cryostat, the voltage was passed through a filter pot. This low-pass filter was a sealed aluminum vessel with cable receptacles that electrically connected to eight $10\text{ M}\Omega$ resistors submerged in Diala oil. The capacitance for the filter was supplied by the cable to the feedthrough. The purpose of the pot was twofold: it reduced the high-frequency ripple from the power supply, and it limited the energy to the TPC in the case of a high voltage discharge.

A feedthrough transmits the high voltage into the cryostat and to the receptacle cup of the cathode plane. This feedthrough is shown in figure 4 and was modeled after the feedthrough used in the ICARUS experiment [4] with a stainless steel inner conductor insulated radially by ultra high molecular weight polyethylene (UHMW PE), and surrounded by a stainless steel ground tube. Grooves were added to the exposed UHMW PE to reduce surface currents. Initially, conducting shielding cups, shown in figure 4b, were installed to reduce the field along the feedthrough. Midway through running, the cups were removed to determine what effect they had on performance. No change was seen. To ensure good electrical contact, the feedthrough has a spring tip that is inserted into a receptacle cup attached to the cathode plane.

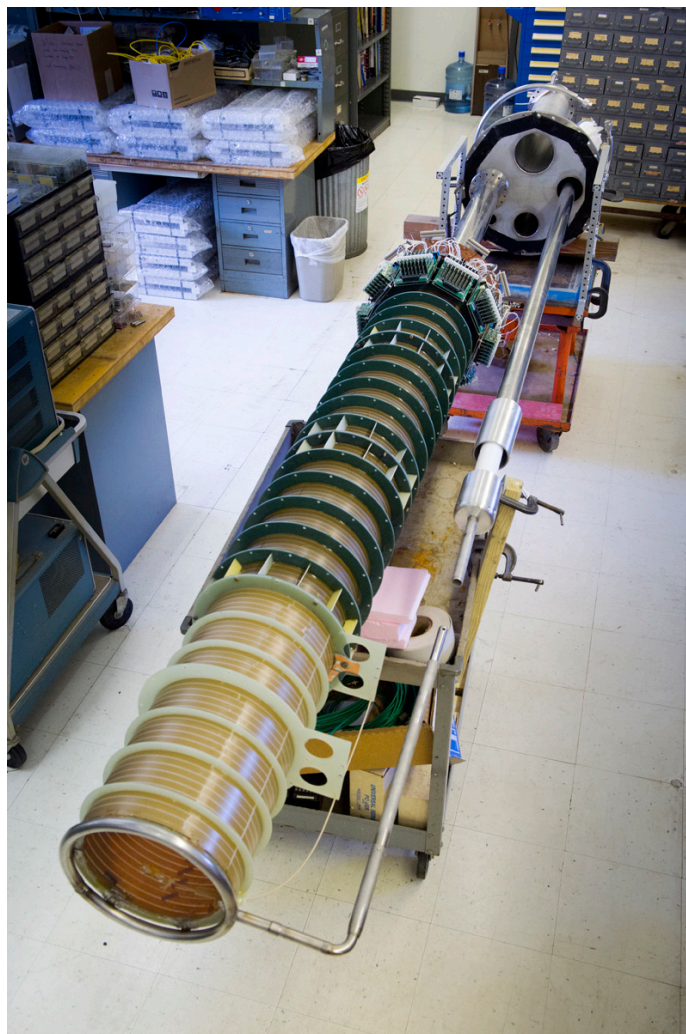


Figure 3: Assembled LongBo TPC.

4. Electronics

4.1 Cold Electronics

The readout electronics used in LongBo are the result of earlier development efforts by MSU for the Bo [2] and ArgoNeuT [5] TPCs. These systems employed preamplifiers positioned outside of the cryostat. The development of cold electronics for a LArTPC was driven by fact that at the 87 K temperature of liquid argon there is less intrinsic noise in a MOSFET preamp than in the best warm preamp. Additionally, by mounting the preamp on the TPC the noise generated by a cable capacitance can be eliminated. A cold MOSFET preamp-filter card was designed and 144 channels were built and deployed on the Bo TPC. In this first application of a MOSFET front-end on a LArTPC, the preamp-filter was implemented with a $2.1 \mu s$ peaking time. These “discrete” MOSFET preamp-filter cards were used on the LongBo LArTPC described in this paper.

A MOSFET ASIC preamp-filter for use at cryogenic temperatures was designed by BNL for



(a)



(b)

Figure 4: Photographs of the HV feedthrough without (a) and with (b) the electric field shielding cups.

LBNE [9]. It is also the readout of the TPC detector for the MicroBooNE experiment [10]. A version (V4) of this 16-channel ASIC became available in 2012 and was implemented for the LongBo TPC. One 16-channel preamp-filter card was modified to use a section of the MicroBooNE motherboard that serviced a single ASIC as a mezzanine board. The input/output connectors, bias-voltage distribution and decoupling capacitors of the card were retained. An ASIC control box was built which set the gain and peaking time parameters of the ASIC. The ASIC modified preamp-filter card was installed in place of one induction plane card with the signals processed by the same digitizing electronics.

4.2 Signal to Noise Ratio

The signal to noise ratio is an important metric of performance for a liquid argon detector. The absolute numerical value depends upon wire spacing, wire capacitance, readout electronics and drift field strength. Because 16 channels of the LongBo readout electronics were instrumented with the BNL ASIC preamplifier, a direct performance comparison can be made between the ASIC version of the preamplifier and the discrete CMOS version used for the remaining channels.

To measure the noise for each channel, a special run of 200 triggers was taken with a random trigger and no drift field. For each channel, the measured ADC counts for all 200 triggers were combined and the distribution fit to a Gaussian function. The width of the best fit Gaussian is reported as the noise in figure 5. The measured noise in Fig. 5 can also be determined from regular data runs with an external muon trigger and nominal drift field if signals from cosmic ray muons are removed from the acquired waveforms.

The signal strength was extracted from straight muon tracks acquired with the cosmic ray muon trigger. The signal to noise ratio of the discrete electronics chain was determined from signals on the collection plane wires. Clean tracks were selected from the first 200 triggers in each run considered using the event display. Only tracks whose projection onto the wire plane under study was nearly perpendicular to wire direction and centered on the wire plane were selected. The signal strength is recorded as the maximum ADC count in the waveform. The outermost two

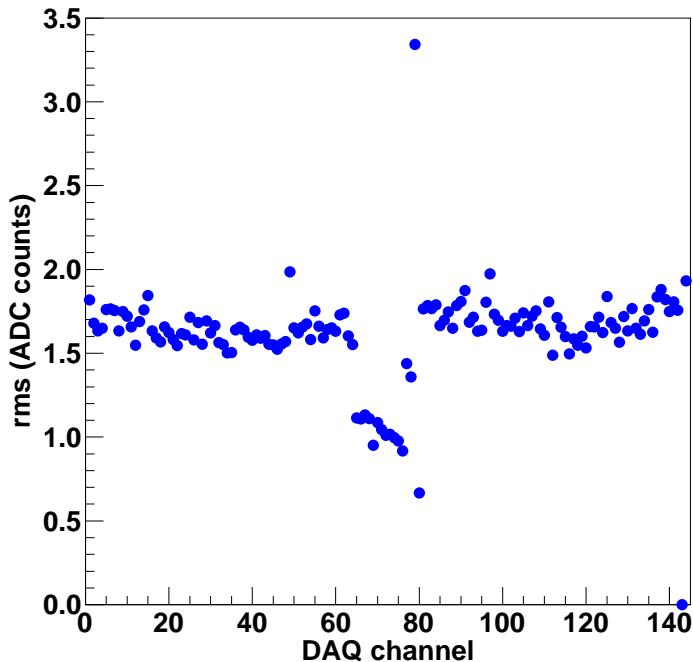


Figure 5: Measured noise as a function of DAQ channel number. Channels 1-48 are the first induction plane, channels 49-96 are the second induction plane and channels 97-144 are the collection plane. Channels 65-80 are instrumented with the BNL ASIC preamplifier, all other channels are instrumented with the MSU discrete CMOS preamplifier. After the first HV breakdown, four channels of the ASIC readout (channels 77-80) exhibited more noise than before and it was no longer possible to change their parameter settings. All of the MSU discrete CMOS channels survived the HV breakdowns.

wires on either edge of the wire plane were excluded from the analysis as a fiducial volume cut intended to reject hits close to the field cage where the drift field may not be uniform and the pulse heights are noticeably reduced. In addition, wires exhibiting pulse heights greater than 1.5 times the average pulse height for the track were interpreted as delta rays and excluded. Finally, wires with more than one hit for a given trigger were excluded.

In the absence of diffusion, the length of the track segment that contributes to the signal on a particular collection plane wire is $\frac{\Delta w}{\sin(\theta)\cos(\phi)}$, where $\Delta w = 4.7$ mm is the wire spacing and θ and ϕ

are the reconstructed track angles defined in § 6.1. The individual measured signal strengths were reduced by a factor of $\sin(\theta)\cos(\phi)$ before taking the average of all *good* collection wire values from the 10-12 event sample to obtain the value of the signal strength $S = 50.3$ ADC counts and a signal to noise ratio of $50.3/1.69 \sim 30$ for the discrete CMOS electronics chain.

The signal to noise ratio provides a good comparison of the performance of the different amplifier flavors. The ASIC preamplifier is connected to the center 16 wires of the middle (induction) wire plane, so induction plane signals must be compared. For these bipolar signals, the signal strength used is the difference between the pedestal and the minimum ADC count of the waveform, or the depth of the dip in the bipolar signal shape. Tracks whose projection onto the middle wire plane is perpendicular to the wire direction were selected ($\phi \sim 60^\circ$) and the extracted signal strengths were normalized by the factor $\sin(\theta)\cos(\phi - 60^\circ)$. The ratio of the average signal strength for ASIC and discrete channels is reported in table 1 for different values of the shaping time constant. Both the measured noise and the signal to noise ratio increase with the shaping time constant.

Table 1: Comparison of signal and noise for discrete CMOS preamplifier and the ASIC preamplifier for different settings of the shaping time constant of the ASIC. The discrete CMOS preamplifiers have a fixed shaping time of $2 \mu\text{s}$. The gain setting of the ASIC was 25 mV/fC for all measurements tabulated.

Shaping time (μs)	S	$S_{discrete}$	N	$N_{discrete}$	$(S/N)/(S/N)_{discrete}$
0.5	10.1	36.1	0.55	1.69	0.9
1.0	19.3	35.1	0.75	1.69	1.2
2.0	33.6	35.5	1.10	1.69	1.4
3.0	40.3	35.8	1.35	1.69	1.4

Figure 6 shows the shape of the amplified signal on a single wire for different shaping times, with the signals scaled to have the same peak height to facilitate comparison. There is little if any difference in the pulse shapes - the shape is dominated by the width of the pulses before amplification. Changing the shaping time constant changes the overall gain of the amplifier.

4.3 Trigger

The presence of a through-going muon was detected by three sets of scintillation counters placed around the exterior of the LAPD tank. Each set consisted of two groups of counters placed on opposite sides of the tank, with the line intersecting the groups of counters passing roughly perpendicular to the wire direction for one wire plane. There were 8 counters (4 pairs) in each of the 6 groups, stacked in a column for an effective area of scintillator roughly 3 m by 0.4 m , for a total of 48 counters. One control and concentrator unit (CCU) controls 48 counters setting the gain of the photomultiplier tube (PMT) and a discriminator threshold [11]. A coincidence was required between counters on opposite side of the tanks, and the track angle coverage is shown in § 6.1.

5. Operation

Figure 7 shows the positions of the TPC and the high voltage feed through inside the LAPD tank.

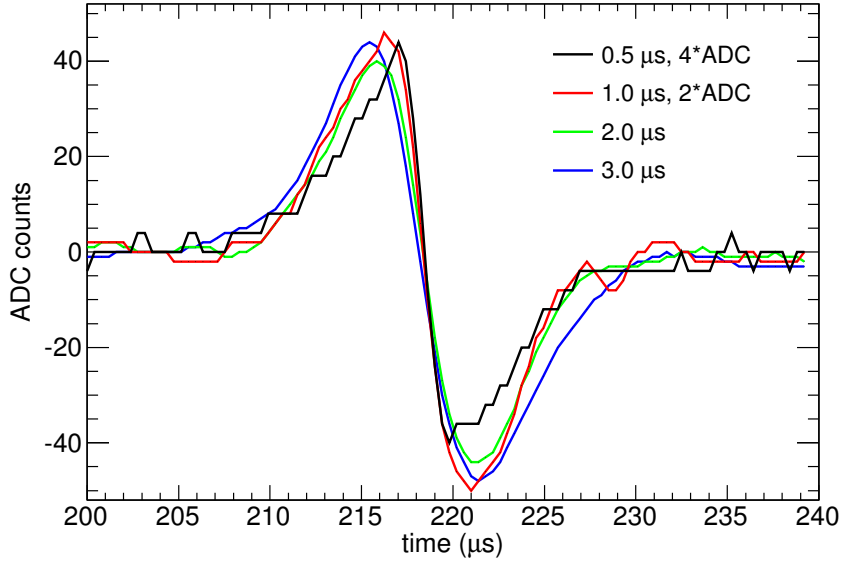


Figure 6: Raw signal shapes for induction plane signals with different settings of the ASIC shaping time constant are shown. The horizontal axis has an arbitrary zero so that the pulses are shown with the zero crossing point artificially aligned. The tracks from which these signals are taken form an angle of roughly 20 degrees with the plane of the wires, or $\theta \sim 70$. The angle between the projection of the track onto the wire plane and the wires themselves is ~ 80 degrees.

After purging the cryostat with argon gas and then filtering the argon gas for several days, as described in [1], the cryostat was filled with liquid argon. The high voltage was raised after the electron drift lifetime passed 0.3 ms. The TPC data taking lasted for 8 months.

An issue we encountered in the LongBo run was that the high voltage was unstable. The cause of the instability is unknown, but was present during the entire data-taking period. This instability forced the running of the TPC at a lower high voltage than desired, ultimately reaching a maximum -75 kV, with occasional trips, instead of the desired 100 kV for a 2 m drift TPC. Even with the lower-than-desired high voltage, several hundred thousand clear cosmic ray muon tracks were recorded. The data were used to study the electronics performance and liquid argon purity.

6. Results

6.1 Measurement of Electron Attenuation Using Cosmic Ray Muons

When cosmic ray muons pass through the liquid argon, they deposit energy through ionization and scintillation. The ionization electrons are drifted by the electric field and collected by the wire planes. The variation of the energy deposition along the muon track is small for the energetic muons. By examining the signal recorded by each wire as a function of electron drift time, one can measure the attenuation of ionization electrons along the drift distance and determine the electron drift lifetime. This method was used by ArgoNeuT to derive an electron drift lifetime [5].

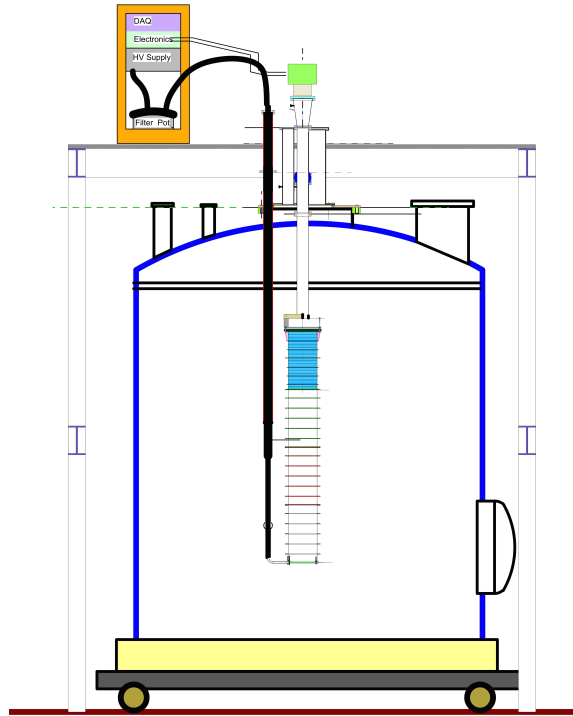


Figure 7: The TPC and high voltage feed through inside the LAPD tank.

We analyzed cosmic ray muon data taken during one full cycle of LAPD running, from when the liquid argon started recirculating through the filters to when it stopped. The high voltage we applied to the cathode was -70 kV during this period, which produced an electric field of 350 V/cm in the TPC volume. In this section, we present results on the measurements of electron attenuation using these data.

There are $491\,966$ triggered events during this run period. We use the LARSOFT software package [12] to reconstruct cosmic ray muon events. The automated reconstruction first converts the raw signal from each wire to unipolar pulse by removing electronics and electric field responses through deconvolution, and then finds hits by fitting a Gaussian to the resulting pulse. The hits from each plane of the TPC are grouped into clusters in drift time and wire number. Three dimensional tracks are constructed from pairs of line-like clusters in each plane. There are $274\,491$ events with at least one reconstructed track. Figure 8 shows one example event where a muon track is visible.

In this analysis we only consider the $223\,194$ events with exactly one reconstructed track that has at least 5 reconstructed 3-dimensional points along the track trajectory. We do not use events with multiple muon tracks because we cannot determine the track start time, t_0 , for each track. Figure 9 shows the angular distributions of the reconstructed tracks. The track angle is determined by the reconstructed track start and end points, assuming the track is a straight line. The zenith angle θ is peaked around 60° and the azimuthal angle ϕ is determined by the trigger counter locations. Figure 10 shows the reconstructed track start point x , in the drift direction, versus the θ angle; $x = 0$ is near the wires. The muons normally enter the TPC in the middle, but they can be

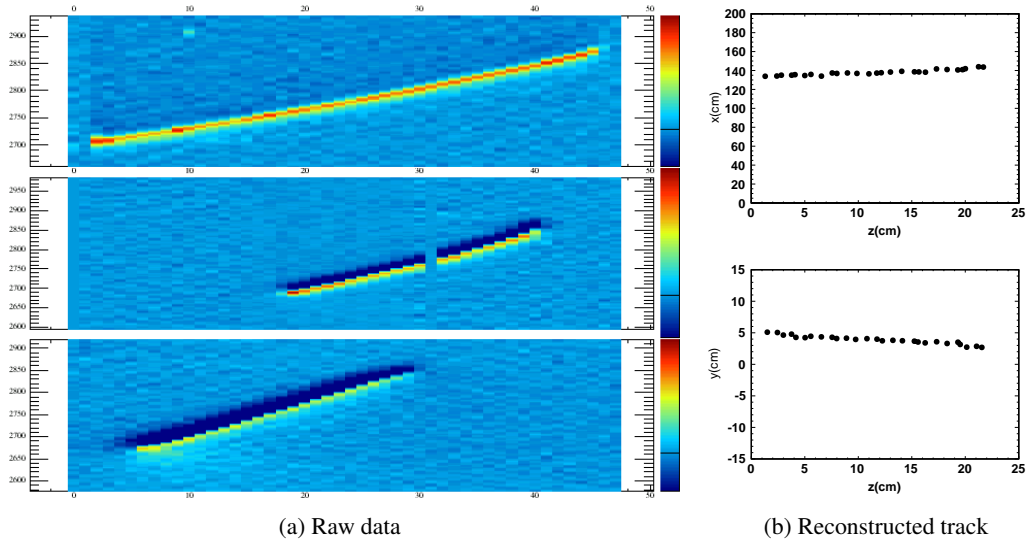


Figure 8: Run 293 Event 2225. (a) Drift time versus wire ID for raw wire signal from 3 wire planes. Red color represents large positive charge and blue color represents large negative charge. (b) Reconstructed track points in the x-z and y-z projections.

close to the wire planes and cathode.

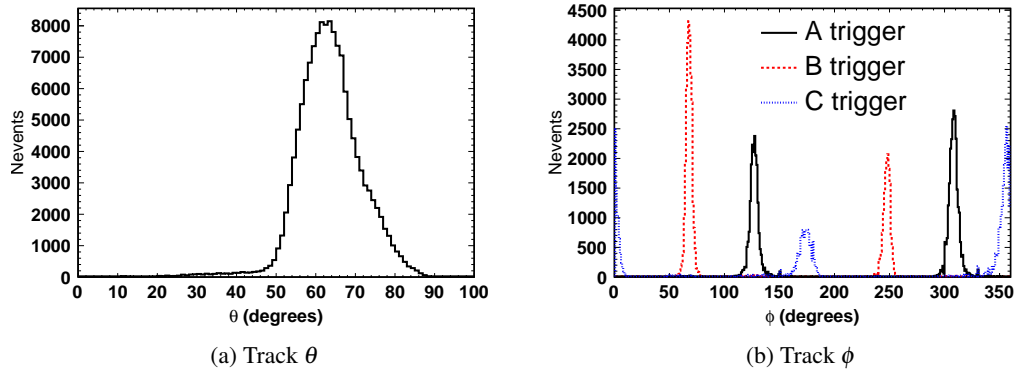


Figure 9: Reconstructed track angles: (a) θ - with respect to the vertical direction, while $\theta = 0$ is at the zenith; (b) ϕ , events taken with different triggers have distinct ϕ distributions.

The determination of the argon purity is performed using the collection plane hits on the track. We first select events with well reconstructed and clean tracks, where

1. the RMS distance of reconstructed 3D points with respect to a straight line determined by track start and end points should be less than 6.3 cm;
2. the number of hits that are not associated with the reconstructed track should be less than 11;
3. track length is required to be greater than 15 cm;

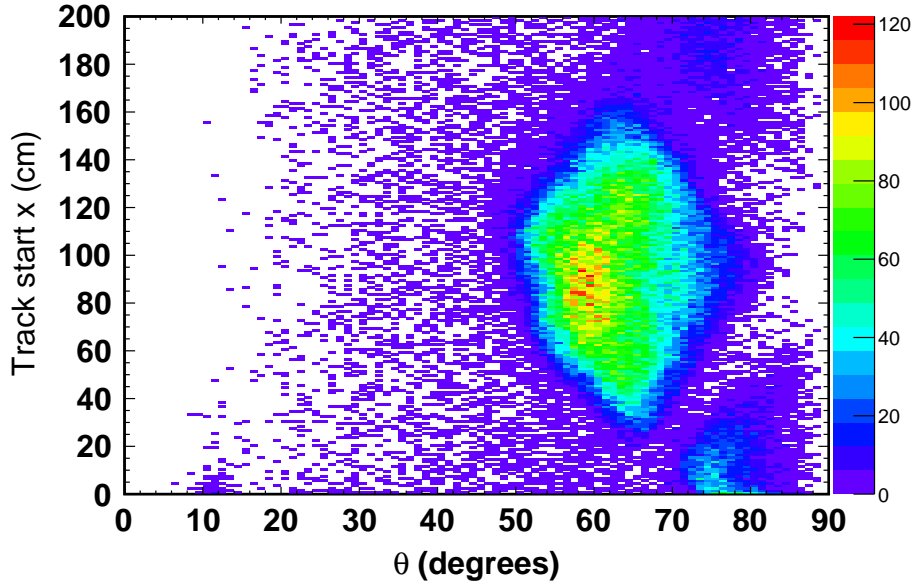


Figure 10: Reconstructed track start point in the drift direction (x) versus track angle (θ). The muons normally enter the TPC in the middle, but they can be close to the wire planes and cathode.

4. track length $\times \cos \phi$, the projection along the collection plane trigger direction, is required to be greater than 10 cm;
5. θ is required to be between 50° and 70° .

The selection was chosen to maximize the good track fraction. We then select all hits on the collection plane associated with the tracks. We require only one hit on each wire. If there is one hit on each of three contiguous wires that has $dQ/dx > 2000$ ADC/cm, we do not use those three hits. This requirement is meant to remove delta rays.

For each selected hit, we look at raw wire signal for that hit in the region $[t - 3 \times \sigma, t + 3 \times \sigma]$, where t is the reconstructed hit time and σ is the reconstructed hit width. We first find the peak of the raw digits in ADC, we then sum all the digits above a threshold of 10% of the peak to get the charge of the hit. This threshold is chosen based on measured signal to noise ratio. By using raw wire signal we remove uncertainties introduced by signal shaping in the hit reconstruction. We then divide the hit charge by the track pitch, which is defined as the wire pitch over dot product of the track direction and the direction normal to the wire direction in the wire plane, to get dQ/dx for the hit.

Figure 11a shows the hit dQ/dx versus electron drift time distribution using data taken in a 2-hour window. This data set is for a poor electron lifetime of ~ 0.4 ms, which corresponds to the first TPC measurement in figure 13. Figure 11b shows the dQ/dx distribution for hits with drift time between 456 and 507 μs , indicated in the left panel. We fit a Landau convoluted with Gaussian function to the dQ/dx distribution. An example fit is shown in figure 11b. Figure 11c shows the most probable value (MPV) from the Landau fit as a function of drift time. The signal decreases as

drift time increases as expected. We fit an exponential function to the data points:

$$dQ/dx = e^{-at_d+b}, \quad (6.1)$$

where t_d is the drift time and a is the attenuation constant. Figure 12 shows $dQ/dx_0 = dQ/dx(t = 0) = e^b$ as a function of time and the fluctuation is small.

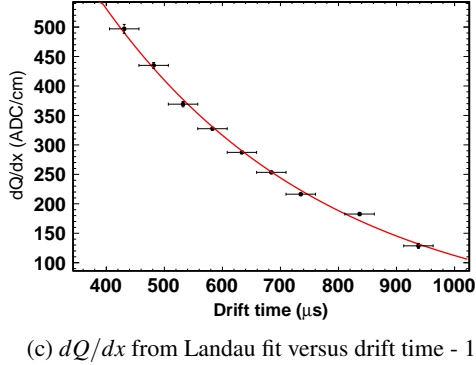
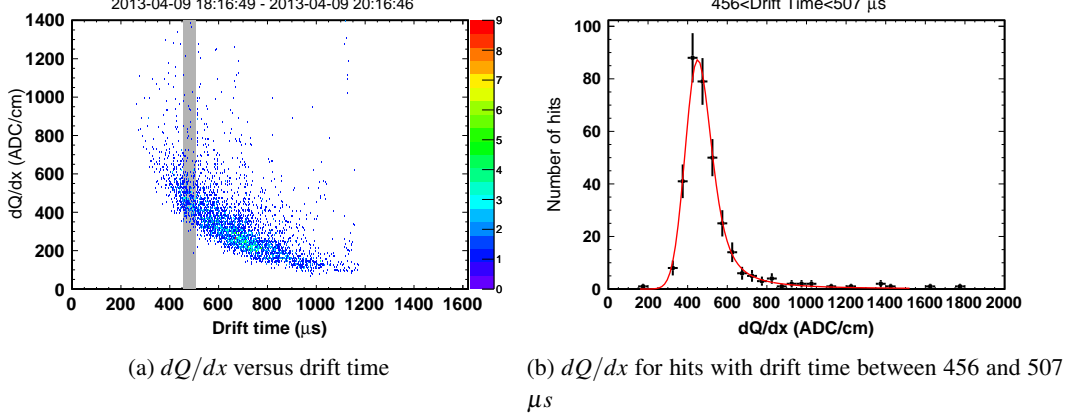


Figure 11: dQ/dx distributions of hits using data taken in a 2-hour window. (a) Scatter plot of dQ/dx as a function of electron drift time; (b) dQ/dx distribution for hits with drift time between 456 and 482 μs ; (c) dQ/dx from Landau fit as a function of drift time.

LAPD reported the measurement of electron attenuation using purity monitors [1]. The result was presented as Q_A/Q_C as a function of time, where Q_A/Q_C represents the fraction of electrons generated at the purity monitor cathode that arrive at the anode. It is determined by the electron drift time (t_d) and electron lifetime (τ) or attenuation constant (a):

$$Q_A/Q_C = e^{-t_d/\tau} = e^{-at_d}. \quad (6.2)$$

In order to compare the measurement using TPC data with the measurement using purity monitors, we calculate the equivalent Q_A/Q_C using the attenuation constant measured by the TPC data and $t_d = 0.31$ ms, which is the electron drift time from the cathode grid to the anode grid in the purity monitor. Figure 13 shows the comparison between Q_A/Q_C measured by the purity monitors and

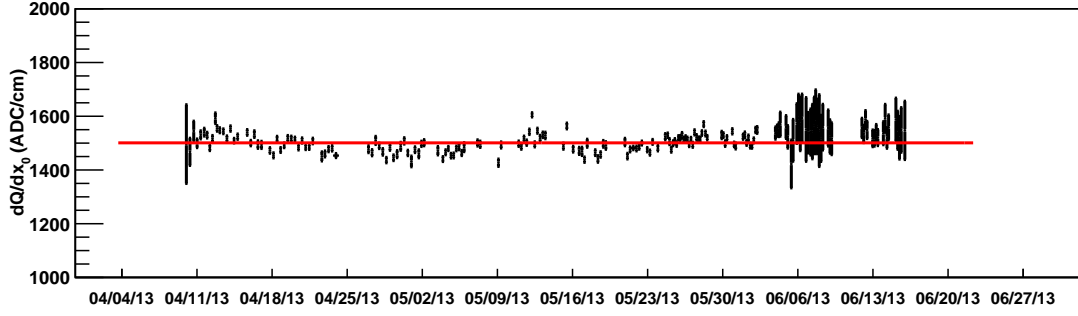


Figure 12: dQ/dx_0 as a function of time.

the calculated Q_A/Q_C using attenuation constant measured using the TPC data. The statistical uncertainties from the original Landau fits are propagated through the attenuation fits to figure 13, and are smaller than the red points. The sources of systematic error on Q_A/Q_C measured by the purity monitor are discussed in Ref. [1] and shown on the plot as a combined 5% absolute uncertainty.

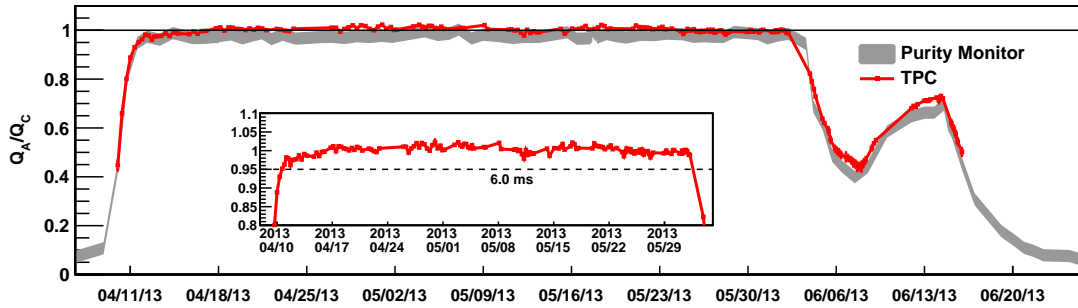


Figure 13: Comparison between Q_A/Q_C measured by the purity monitors and the calculated Q_A/Q_C using attenuation constant measured using the TPC data. The details of the TPC results are shown in the inset compared with the value $Q_A/Q_C = 0.95$ which corresponds to electron drift lifetime $\tau = 6$ ms. Over the 1.5 months the Q_A/Q_C from TPC measurements never gets larger than 1.03, and tracks the purity monitor's behavior for lower Q_A/Q_C .

The TPC measurement confirms the conclusion that the electron drift lifetime is greater than 6 ms [1]. The attenuation measured by the TPC is consistently smaller than the measurement using purity monitors. This result may be caused by the possibility that some of the drifting electrons are not collected at the anode of the purity monitor that we used for the measurement. Over a long period of time, the attenuation is negligible in the TPC measurement. Occasionally we observe a slight increase of dQ/dx at longer drift time, which manifests Q_A/Q_C slightly above 1. We have investigated many systematic effects that can cause this result. The possible causes of this result include the distortion of electric field resulting from the presence of positive ions in the TPC volume, the instability of high voltage discussed in the next section, or extraction of charge from the pulse shape which can be affected by physics processes such as the muon multiple scattering or the drifting electron diffusion.

6.2 High Voltage Stability

The TPC's resistive chain was likely damaged before data taking began. The power supply was set to turn off if it drew an over-current much greater than twice the operating current of the TPC. During data taking, the cathode high voltage never sustained greater than 80 kV for a significant period with most data being collected with 60 or 70 kV on the cathode. A correlation was noted between greater high voltage stability and greater electronegative contamination in the argon. This trend can be seen in figure 14 where the number of high voltage trips is displayed along with a purity monitor reading as a function of time. While a precise characterization of the dependence is beyond the scope of this paper, the behavior agrees with other studies in the literature that have shown a trend between an increase in electronegative contamination and an increase in liquid argon's dielectric strength [6, 7, 8].

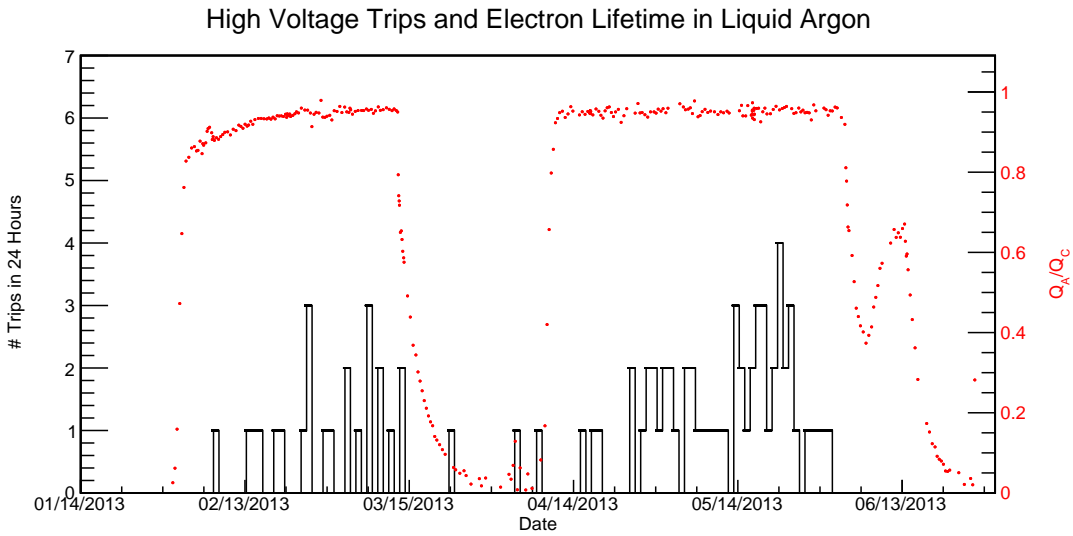


Figure 14: The number of cathode high voltage trips in a 24 hour period and purity monitor values during data taking. The trip counts are given by the black solid line and scale on the left. Trips related to testing the high voltage system were not included in the trip count. A quantification of the argon purity is given by the red dots and the scale on the right.

7. Conclusions

In this paper we have discussed the design and operation of the LongBo TPC in the LAPD cryostat. A ratio $S/N = 50.5/1.69 \sim 30$ was measured for the wires in the collection plane with discrete CMOS electronics. For these data the TPC was operated with a drift field of 350 V/cm. The measured S/N ratio for the ASIC channels was 1.44 times larger than that measured for the discrete channels for the ASIC shaping time of 2.0 μ s and a gain setting of 25 mV/fC. The liquid argon purity measurement using cosmic ray muons in the TPC confirms the previous result using purity monitors that the electron drift lifetime is at least 6 ms. We also observe a correlation between the voltage stability and the liquid argon purity.

Acknowledgments

This work was supported by the US DOE, and by the NSF through Grants 1068318 and 1410972, to Michigan State University. We thank the staff at Fermilab for their technical assistance in running the LAPD experiment. Fermilab is operated by Fermi Research Alliance, LLC under Contract No. De-AC02-07CH11359 with the United States Department of Energy.

References

- [1] M. Adamowski et al., *The Liquid Argon Purity Demonstrator*, 2014 *JINST* **9** P07005.
- [2] C. Bromberg, *First neutrino physics results of the ArgoNeuT experiment, and first tracks with CMOS preamplifiers operating at 87 K*, in Proceedings of the 2nd International Workshop towards the Giant Liquid Argon Charge Imaging Experiment (GLA2011), 5-10 Jun 2011, Jyväskylä, Finland, lartpc-docdb.fnal.gov/0008/000819/001/CBromberg_GLA2011_Proc.pdf, to be published.
- [3] Glassman High Voltage Inc., PO Box 317, 124 West Main Street, High Bridge, NJ 08829-0317, U.S.A. www.glassmanhv.com.
- [4] S. Amerio et al. (ICARUS Collaboration), *Design, construction and tests of the ICARUS T600 detector*, *Nucl. Instrum. Meth. A* **527**, (2004) 329.
- [5] C. Anderson et al. (ArgoNeuT Collaboration), *The ArgoNeuT detector in the NuMI low-energy beam line at Fermilab*, 2012 *JINST* **7** P10019.
- [6] D. Swan and T. Lewis, *Influence of electrode surface conditions on the electrical strength of liquified gases*, *J. Electrochem. Soc.* **107** (1960) 180.
- [7] A. Blatter et al., *Experimental study of electric breakdowns in liquid argon at centimeter scale*, 2014 *JINST* **9** P04006.
- [8] R. Acciarri et al., *Liquid argon dielectric breakdown studies with the MicroBooNE purification system*, 2014 *JINST* **9** P11001.
- [9] C. Adams et al. (LBNE Collaboration), *The Long-Baseline Neutrino Experiment: exploring fundamental symmetries of the universe*, [hep-ex/1307.7335](https://arxiv.org/abs/hep-ex/1307.7335).
- [10] <http://www-microboone.fnal.gov/publications/TDRCD3.pdf>.
- [11] C. Bromberg, *Gain and threshold control of scintillation counters in the CDF muon upgrade for Run II*, *Int. J. Mod. Phys. A* **16S1C** (2001) 1143.
- [12] <https://cdcv.sfnal.gov/redmine/projects/larsoft>. We use version v02_00_01 of this software package.